SHIMADZU
Excellence in Science

Application Note

No. 75

Life Science

Visualization of Lanthanum Precipitates in Gastric Tissue by Laser Ablation-Inductively Coupled Plasma-Mass Spectrometry Imaging

S. Shimma [*1,*2,*3], K. Okuda [*4]

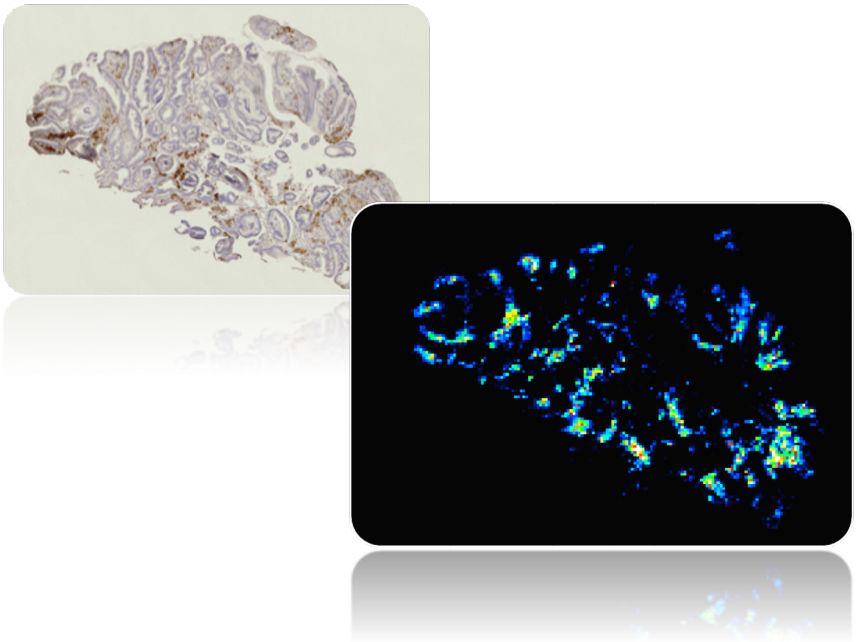

Life Science

■ Abstract

Various applications of mass spectrometry imaging (MS imaging) using laser ablation-inductively coupled plasma-mass spectroscopy (LA-ICP-MS) as a method for imaging metals in living organisms have been reported in recent years. Among those applications, LA-ICP-MS is frequently used in pharmacokinetic analysis and toxicity evaluation of drugs that contain metals. This Application Note reports the results of visualization of the distribution of lanthanum in gastric tissue by LA-ICP-MS, using biopsy specimens from a patient who developed gastritis after administration of lanthanum carbonate.

1. Introduction

In recent years, MS imaging of metals using LA-ICP-MS has attracted attention in many research fields, including basic biology and toxicology. The most important advantage of imaging by LA-ICP-MS is that it can provide high quantitativity in a broad dynamic range because various elements that exist on the tissue surface can be ionized simultaneously with high efficiency.

For this reason, a variety of reports on MS imaging of metals using LA-ICP-MS have been published on topics such as the distribution of endogenous metals in animal and human tissues [1)-3)], research on the toxicity of cadmium in the rat placenta [4)], the effects of dibutyltin on placental and fetal toxicity in rats [5)], and research on lead poisoning in seabirds [6)].

Together with research of this type, pharmacokinetic and toxicological studies on pharmaceuticals that contain metals are also an important application field for LA-ICP-MS imaging [7)-11)]. Alkali metals, alkaline earth metals, and transition metals are used in drug development. In particular, many reports have examined LA-ICP-MS drug MS imaging of anti-cancer agents such as Cisplatin, in which the transition metal platinum (Pt) is used to inhibit DNA synthesis. Many of those studies investigated the connection between platinum formulations and nephrotoxicity by visualization of the distribution of Pt in kidney tissue. To date, however, reports have been largely limited to animal model studies, and only a few studies involving visualization of metals in human clinical samples by LA-ICP-MS have appeared [12)].

In this Application Note, lanthanum (^{139}La) in human gastric biopsy tissue was visualized using a combination of a laser ablation system and a Shimadzu ICPMS-2030. Lanthanum is contained in Fosrenol (lanthanum carbonate hydrate compound), which is used to treat the high-phosphorus blood disease called hyperphosphatemia, and it has been reported that this drug causes gastric inflammation (hemorrhagic gastritis) as the main side effect in the digestive organs. Here, visualization of ^{139}La was carried out, and the results were compared with the immunohistochemistry (IHC) observation results. The results confirmed that a high accumulation of ^{139}La was present in macrophage-positive regions visualized by using the anti-CD68 antibody.

[*1] Department of Biotechnology, Graduate School of Engineering, Osaka University
[*2] Osaka University Shimadzu Omics Innovation Research Laboratories
[*3] Institute for Open and Transdisciplinary Research Initiatives, Osaka University
[*4] Solutions COE, Analytical & Measuring Instruments Division, Shimadzu Corporation

2. Experiment and Techniques

Reagents

Anti-CD68 antibody, 1 × Tris Buffered Saline with Tween® 20, SignalStain® Antibody Diluent, SignalStain® Boost IHC Detection Reagents, and SignalStain® DAB Substrate Kit were purchased from Cell Signaling Technology, Inc. (Danvers, MA, USA). Xylene, a mounting agent, Mayer's hematoxylin solution, and 1 % eosin Y solution were purchased from FUJIFILM Wako Pure Chemical Corporation (Osaka, Japan). Goat serum was purchased from Merck KGaA (Darmstadt, Germany).

Clinical Specimens

Specimens were taken from a patient with symptoms of hemorrhagic gastritis during gastric biopsies performed at Oka Hospital (Honjo, Saitama Prefecture). Written informed consent procedures were followed, and the biopsy specimens were used in this study with the full agreement of the patient. The specimens were anonymized, and after tissue formalin-fixation, the sampled tissue was stored as paraffin-embedded tissue specimens (FFPE blocks).

Sectioning

Sections with a thickness of 8 µm were prepared by slicing the FFPE blocks with a rotary microtome (RM2145, Leica, Wetzlar, Germany), and the sections were then collected on ordinary slide glasses (Matsunami Glass Ind., Ltd. Osaka, Japan) in a water bath at 40 ˚C. After collecting, the slide glasses were allowed to stand on a hot plate (Sakura Finetek Japan, Tokyo, Japan) overnight at 37 ˚C to dry and fix the samples. In this study, serial sections were prepared and used for MS imaging using LA-ICP-MS, IHC staining, and hematoxylin and eosin (H&E) staining.

Deparaffinization

Deparaffinization was performed by 3 cycles of washing (25 ˚C, 5 min) in xylene. The sample for the LA-ICP-MS analysis was only washed with xylene and dried. The samples for IHC or H&E staining were also washed with 100 % ethanol (10 min, 2 cycles), 95 % ethanol (10 min, 2 cycles), and water (5 min, 2 cycles), and were then stained after washing.

Preparation of Quantitative Analysis Samples

In conducting the quantitative analysis, a calibration curve was prepared by the method proposed by Lohöfer et al. [13]. The La standard sample (lanthanum chloride heptahydrate, 99.9 %, 126-03352, FUJIFILM Wako Pure Chemical Corp.) was prepared with gelatin (077-03155, FUJIFILM Wako Pure Chemical Corp.) so as to obtain final concentrations of 90, 450, 900, and 3600 µg/g. The gelatin solutions containing La were then poured into No. 2 cryomolds (Sakura Finetek Japan, Tokyo, Japan) and frozen at -80 ˚C. After freezing, sections with a thickness of 8 µm were prepared from the frozen blocks using a cryomicrotome (CM1950S, Leica, Wetzlar, Germany) and mounted on slide glasses as shown below in Fig. 2(a).

LA-ICP-MS Imaging Experiment and Analysis

The instruments used in this study were an ICPMS-2030 (Shimadzu Corporation) as the ICP-MS and an LSX-213 G2+ laser ablation system (Teledyne CETAC Technologies). The appearance of the instruments is shown in Fig. 1(a). As shown in the schematic system diagram in Fig. 1(b), samples which had been decomposed by the laser ablation system were introduced directly into the ICP and measured with the mass spectrometer. Table 1 shows the ICP-MS and laser ablation conditions. The MS imaging data analysis software IMAGEREVEAL™ MS (Shimadzu Corp.) was used in data display and quantitative analysis.

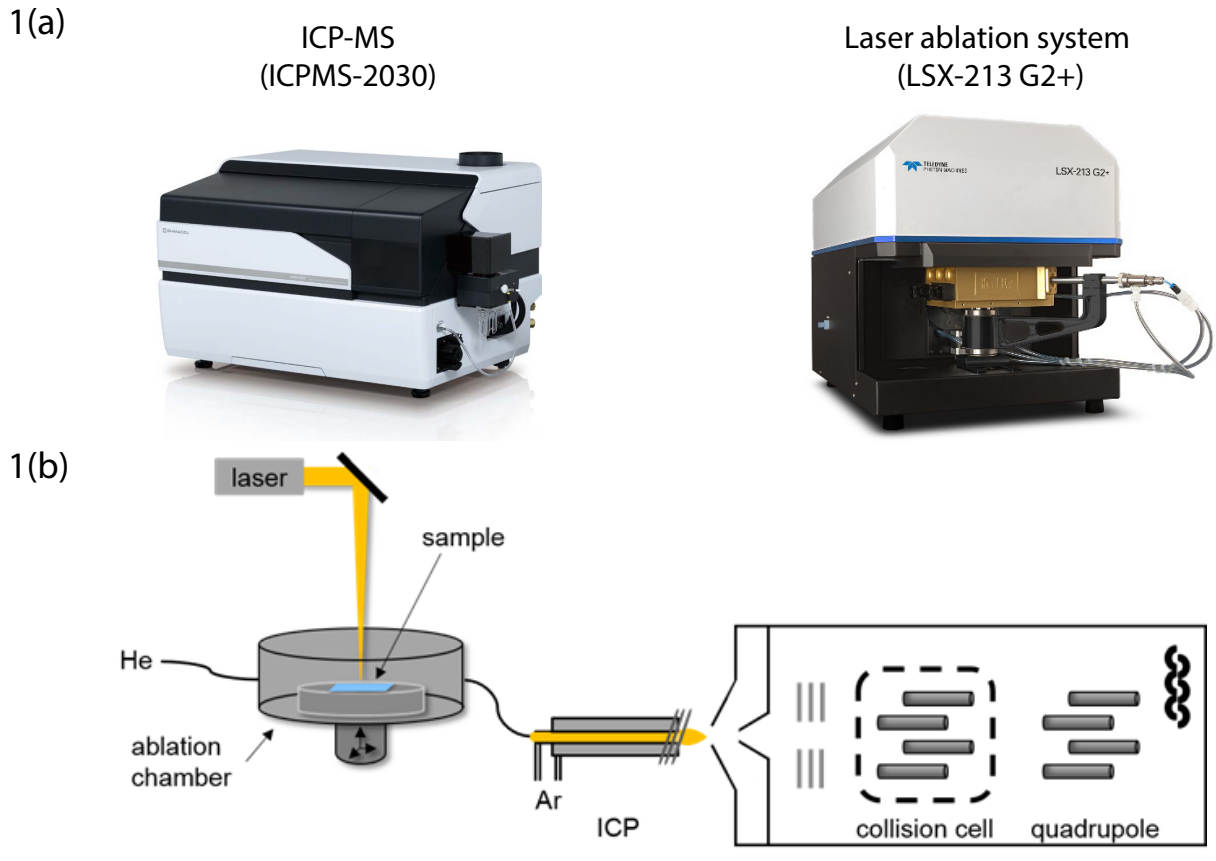

Fig. 1 Instruments Used in Experiment and System Outline
(a) ICPMS-2030 and LSX-213 G2+ Laser Ablation System,
(b) Schematic Diagram of the System

Table 1 Experimental Conditions of ICPMS-2030 and LSX-213 G2+

ICP-MS (ICPMS-2030)	
RF power (kW)	: 1.2
Sampling Depth (mm)	: 5.0
Plasma Gas (L/min)	: 9.0
Auxiliary Gas (L/min)	: 0.70
Carrier Gas (L/min)	: 0.40
Chamber Temperature (˚C)	: 5
Peristaltic Pump Rotation Speed (r.p.m.)	: 20

Laser (LSX-213 G2+, Teledyne CETAC Technologies)	
Repetition frequency (Hz)	: 20
Spot size (µm)	: 15
Scan speed (µm/s)	: 15
He carrier gas (L/min)	: 0.8

3. Results

Comparison of La Distribution and IHC Stained Image Using CD68

Fig. 2(a) shows the IHC observation results with the anti-CD68 antibody using serial sections, and Fig. 2(b) shows the La distribution obtained by MS imaging. It can be understood that the CD68-positive areas (regions shown in brown) are localized and are not distributed over the full tissue area.

On the other hand, La is distributed in a granular form over the entire tissue area. Comparing the two, the positions of La accumulation and the CD68-positive areas are in good agreement. In other words, an inflammatory response occurred in the areas where La had accumulated, suggesting a linkage between the gastritis and the accumulation of La.

As noted previously, it is possible to measure various elements simultaneously by LA-ICP-MS. Therefore, in this experiment, the distribution of phosphorus (P) was also visualized at the same time, as shown in Fig. 2(c). Fig. 2(d) shows the results of overlaying the obtained distributions of La and P, revealing that P is localized in areas where La is localized (white parts show the areas of co-localization).

Fosrenol (lanthanum carbonate hydrate compound), which is a therapeutic drug used to treat hyperphosphatemia, bonds with dietary phosphorus in the intestinal tract and is then excreted from the body in the form of lanthanum phosphate. (https://pharma-navi.bayer.jp/fosrenol/product/moa)

Since it is also known that lanthanum carbonate has a high phosphorus elimination rate, which is independent of pH, it is thought that it also bonds with P in the stomach to form lanthanum phosphate.

Based on these facts, it can be inferred that La does not accumulate as lanthanum carbonate at positions where an inflammation response occurs, but rather, accumulates in the form of lanthanum phosphate.

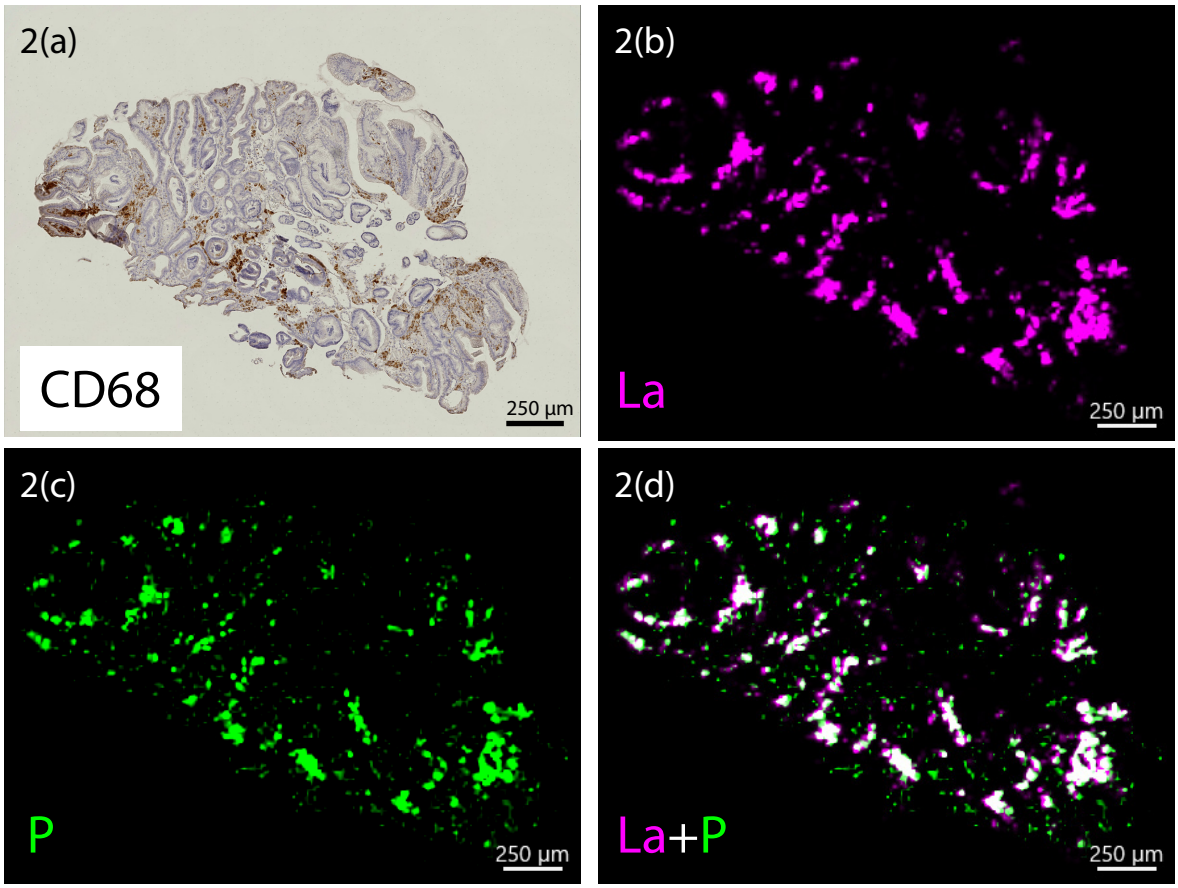

Fig. 2 IHC Observation Results Using Anti-CD68 Antibody and Imaging Results
(a) IHC Observation Results Using Anti-CD68 Antibody,
(b)-(d) Imaging Results of Lanthanum (La), Phosphorus (P), and Overlay of La and P

Study of Calibration Curve

The calibration curve samples prepared by the method shown in Fig. 3(a) were measured under the conditions in Table 1, which were the same as those used in the analysis of the tissue sections. Using IMAGEREVEAL MS, a calibration curve was prepared from the obtained data, as shown in the graph in Fig. 3(b), where the x-axis represents the concentration and the y-axis is the intensity.

From Fig. 3, it can be understood that the calibration curve displays good linearity within the region of the prepared samples. Since the data obtained by this LA-ICP-MS system can be output in a format that can be read directly by IMAGEREVEAL MS, the data analysis was also extremely easy.

3(a)

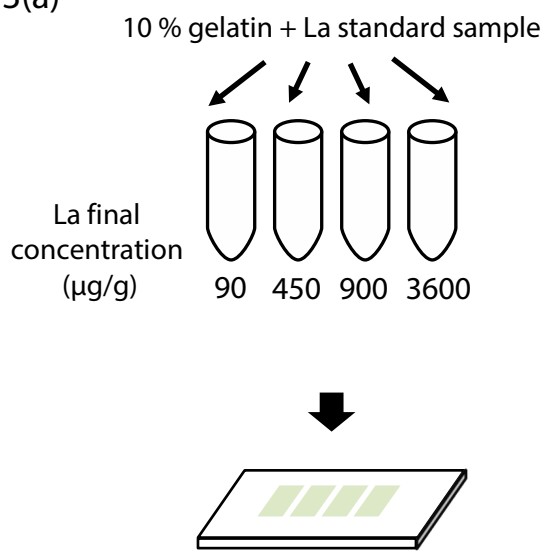

3(b)

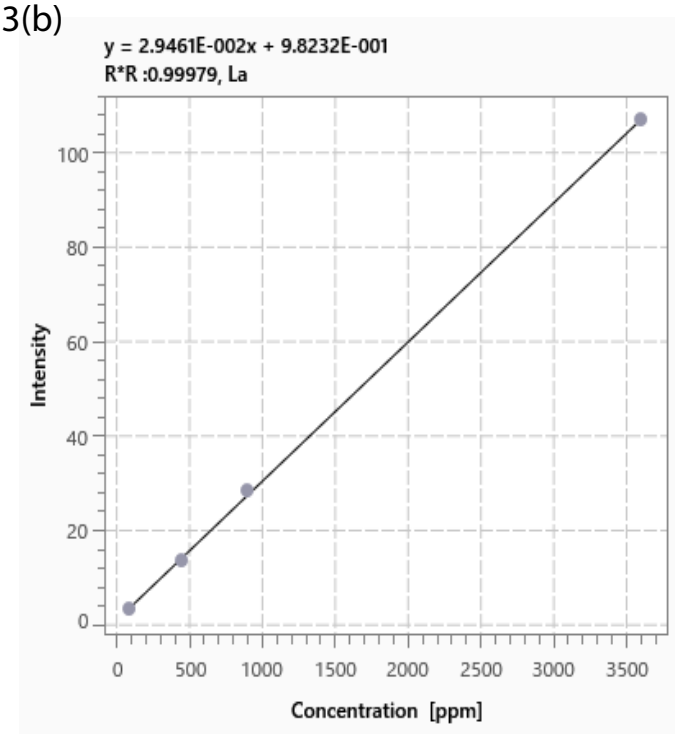

3(c)

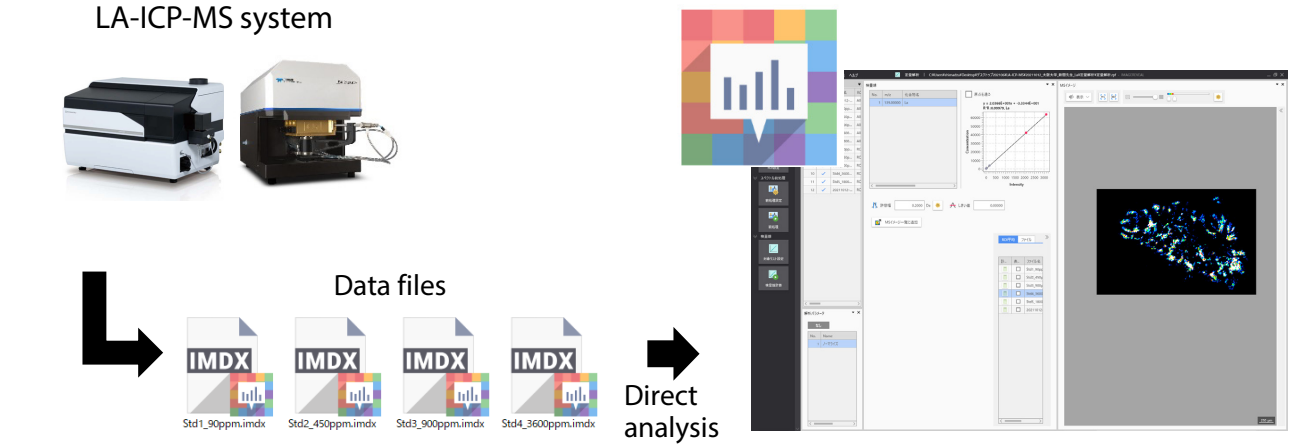

Fig. 3 Calibration Curve in Experiment
(a) Method of Sample Preparation for Calibration Curve,
(b) Calibration Curve Prepared by IMAGEREVEAL MS,
(c) Workflow from Data Output to Analysis

Quantitative MS Imaging Results

Next, the amount of accumulated La in the accumulation areas was investigated using the calibration curve obtained in Fig. 3(b). If IMAGEREVEAL MS is used, imaging images with quantitative information can be generated easily by applying the regression equation obtained with the calibration curve to the intensity distribution on the actual tissue. Regions of interest (ROI) can be prepared from the quantitative MS imaging results obtained in this manner, and the quantitative values in the ROI can be determined. Here, in the La distribution shown in Fig. 3(b), arbitrary accumulation areas were selected as the ROIs in Fig. 4(a), and the amount of La accumulation in those areas was investigated. Fig. 4(b) shows the obtained quantitative results as dot plots. The concentration range in the La accumulation areas was from approximately 3.0×10^4 ppm to 6.5×10^4 ppm, and the average value was $4.0 \times 10^4 \pm 0.9$ ppm.

In this experiment, it was difficult to prepare sections of the calibration curve samples with high concentration exceeding 1.0×10^4 ppm similar to those of the low concentration calibration curve samples. However, the quantitative values were calculated by extrapolating the calibration curve, as the ICPMS-2030 used in this experiment can provide good linearity in the intensity region corresponding to a 4 % La concentration.

Microscopic Observation of La Accumulation Areas

Due to the extremely low solubility of lanthanum phosphate, there is a possibility that crystals originating from lanthanum phosphate in the La accumulation areas can be observed by microscope. Here, H&E staining of serial sections was performed, and the area with the highest concentration of La was observed with a microscope. Fig. 5(a) shows the observation area, and Fig. 5(b) shows the image captured by microscopic observation in this area (objective lens magnification: 40x). Numerous brown-colored precipitates were observed in the interior area indicated by the rectangle in Fig. 5(b). In addition to the areas shown here, the same type of brown precipitates were also confirmed in other La accumulation areas.

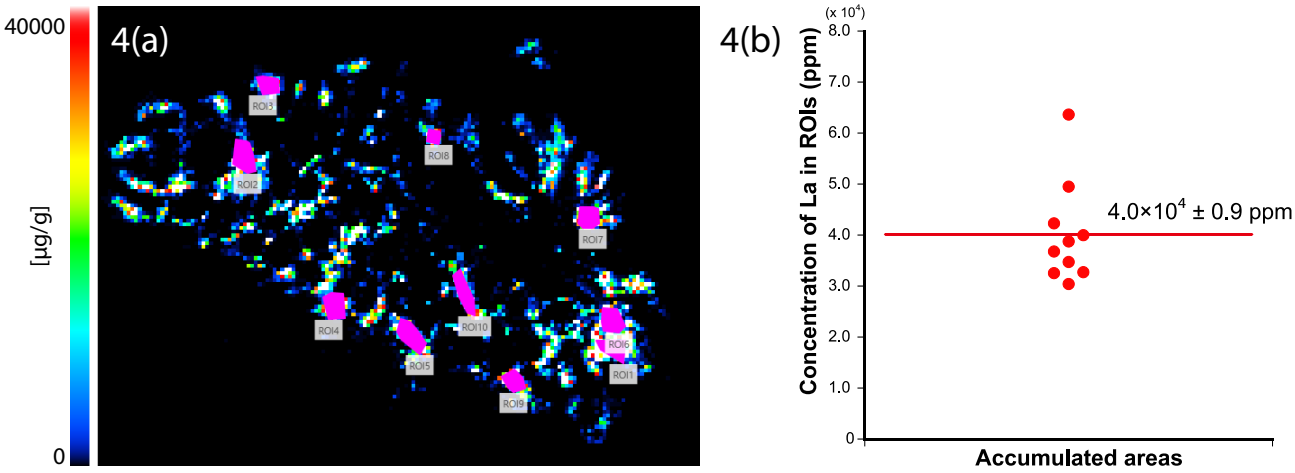

Fig. 4 Quantitative Analysis Results
(a) ROIs on the Obtained Quantitative Image Set by IMAGEREVEAL MS,
(b) Dot Plots of La Concentrations Calculated from the ROIs

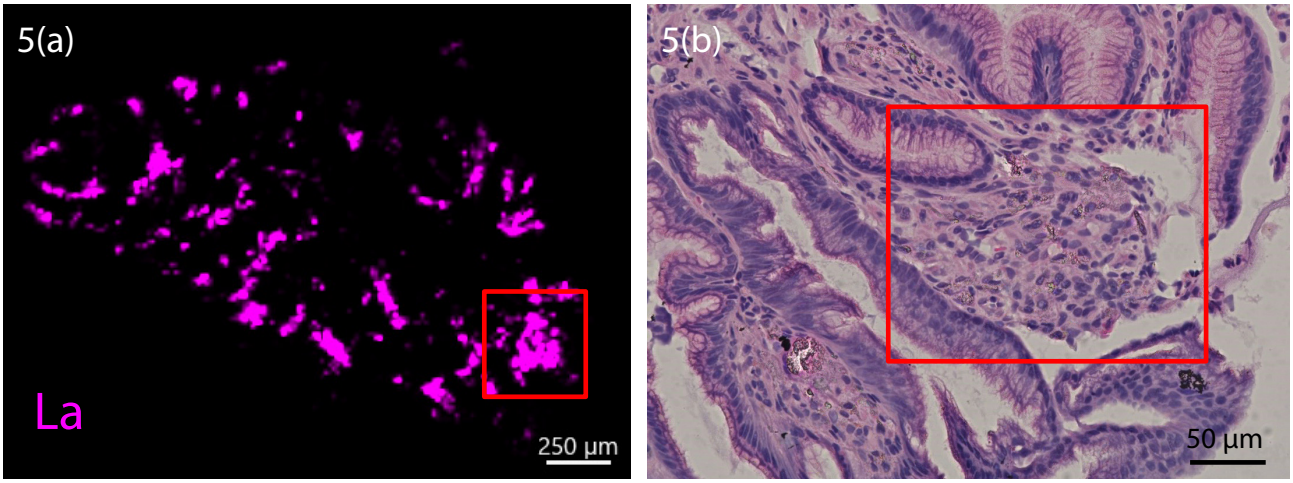

Fig. 5 Results of H&E Staining in Localized Areas
(a) Observation Area in La Imaging Result (Area in Red Square),
(b) Microscopic Observation Image of H&E Stained Section in the Region Set in (a)

4. Conclusion

In this Application Note, lanthanum in gastric tissue was visualized by LA-ICP-MS using a Shimadzu ICPMS-2030. The average La concentration was 4×10^4 ppm, and because P was also co-localized in areas where La had accumulated, it is thought that La precipitated in the form of lanthanum phosphate. Based on a comparison with the immunohistochemistry (IHC) obtained with the anti-CD68 antibody, which detects markers expressed by macrophages, it is considered that an inflammation response occurs in La accumulation areas because the specimens were also CD68-positive in La localization areas. La accumulation areas were also observed in H&E stained tissues, and crystal-like precipitates were observed in those areas. In the future, the importance of applications in which LA-ICP-MS is used to acquire information that cannot be obtained by pathological staining alone is expected to increase accompanying the development of various new metallic preparations.

Acknowledgment

The authors wish to take this opportunity to express their appreciation to Dr. Kazuto Kojima (Keisuikai Oka Hospital) for providing the specimens and Ms. Hiromi Saito (Project Researcher, Osaka University Graduate School of Engineering) for carrying out the sample preparation work in the course of this experiment.

<References>

1) Zoriy, M. V.; Dehnhardt, M.; Reifenberger, G.; Zilles, K.; Becker, J. S., Imaging of Cu, Zn, Pb and U in human brain tumor resections by laser ablation inductively coupled plasma mass spectrometry. International Journal of Mass Spectrometry 2006, 257 (1), 27-33.
2) Becker, J. S.; Zoriy, M.; Becker, J. S.; Dobrowolska, J.; Matusch, A., Laser ablation inductively coupled plasma mass spectrometry (LA-ICP-MS) in elemental imaging of biological tissues and in proteomics. Journal of Analytical Atomic Spectrometry 2007, 22 (7).
3) Becker, J. S.; Zoriy, M.; Matusch, A.; Wu, B.; Salber, D.; Palm, C.; Becker, J. S., Bioimaging of metals by laser ablation inductively coupled plasma mass spectrometry (LA-ICP-MS). Mass Spectrom. Rev. 2010, 29 (1), 156-75.
4) Yamagishi, Y.; Furukawa, S.; Tanaka, A.; Kobayashi, Y.; Sugiyama, A., Histopathological localization of cadmium in rat placenta by LA-ICP-MS analysis. J. Toxicol. Pathol. 2016, 29 (4), 279-283.
5) Furukawa, S.; Tsuji, N.; Kobayashi, Y.; Yamagishi, Y.; Hayashi, S.; Abe, M.; Kuroda, Y.; Kimura, M.; Hayakawa, C.; Sugiyama, A., Effect of dibutyltin on placental and fetal toxicity in rat. J. Toxicol. Sci. 2017, 42 (6), 741-753.
6) Ishii, C.; Nakayama, S. M. M.; Kataba, A.; Ikenaka, Y.; Saito, K.; Watanabe, Y.; Makino, Y.; Matsukawa, T.; Kubota, A.; Yokoyama, K.; Mizukawa, H.; Hirata, T.; Ishizuka, M., Characterization and imaging of lead distribution in bones of lead-exposed birds by ICP-MS and LA-ICP-MS. Chemosphere 2018, 212, 994-1001.
7) Moreno-Gordaliza, E.; Giesen, C.; Lazaro, A.; Esteban-Fernandez, D.; Humanes, B.; Canas, B.; Panne, U.; Tejedor, A.; Jakubowski, N.; Gomez-Gomez, M. M., Elemental bioimaging in kidney by LA-ICP-MS as a tool to study nephrotoxicity and renal protective strategies in cisplatin therapies. Anal. Chem. 2011, 83 (20), 7933-40.
8) Bonta, M.; Lohninger, H.; Laszlo, V.; Hegedus, B.; Limbeck, A., Quantitative LA-ICP-MS imaging of platinum in chemotherapy treated human malignant pleural mesothelioma samples using printed patterns as standard. J. Anal. At. Spectrom. 2014, 29 (11), 2159-2167.
9) Egger, A. E.; Theiner, S.; Kornauth, C.; Heffeter, P.; Berger, W.; Keppler, B. K.; Hartinger, C. G., Quantitative bioimaging by LA-ICP-MS: a methodological study on the distribution of Pt and Ru in viscera originating from cisplatin- and KP1339-treated mice. Metallomics 2014, 6 (9), 1616-25.
10) Schreiber-Brynzak, E.; Pichler, V.; Heffeter, P.; Hanson, B.; Theiner, S.; Lichtscheidl-Schultz, I.; Kornauth, C.; Bamonti, L.; Dhery, V.; Groza, D.; Berry, D.; Berger, W.; Galanski, M.; Jakupec, M. A.; Keppler, B. K., Behavior of platinum(iv) complexes in models of tumor hypoxia: cytotoxicity, compound distribution and accumulation. Metallomics 2016, 8 (4), 422-33.
11) Van Acker, T.; Van Malderen, S. J. M.; Van Heerden, M.; McDuffie, J. E.; Cuyckens, F.; Vanhaecke, F., High-resolution laser ablation-inductively coupled plasma-mass spectrometry imaging of cisplatin-induced nephrotoxic side effects. Anal. Chim. Acta 2016, 945, 23-30.
12) Shimma, S.; Makino, Y.; Kojima, K.; Hirata, T., Quantitative Visualization of Lanthanum Accumulation in Lanthanum Carbonate-Administered Human Stomach Tissues Using Mass Spectrometry Imaging. Mass Spectrom (Tokyo) 2020, 9 (1), A0086.
13) Lohofer, F.; Buchholz, R.; Glinzer, A.; Huber, K.; Haas, H.; Kaissis, G.; Feuchtinger, A.; Aichler, M.; Sporns, P. B.; Holtke, C.; Stolting, M.; Schilling, F.; Botnar, R. M.; Kimm, M. A.; Faber, C.; Walch, A. K.; Zernecke, A.; Karst, U.; Wildgruber, M., Mass Spectrometry Imaging of atherosclerosis-affine Gadofluorine following Magnetic Resonance Imaging. Sci. Rep. 2020, 10 (1), 79.

SHIMADZU
Shimadzu Corporation
www.shimadzu.com/an/

First Edition: Jun. 2022